УДК 539.165

FIRST EVIDENCE FOR NEUTRINOLESS DOUBLE BETA DECAY

H. V. Klapdor-Kleingrothaus [a1], *A. Deitz* [a], *I. V. Krivosheina* [a,b]

[a] Max-Planck-Institut für Kernphysik, Postfach 10 39 80, D-69029 Heidelberg, Germany

[b] Radiophysical-Research Institute, Nizhny Novgorod, Russia

The data of the HEIDELBERG–MOSCOW double beta decay experiment for the measuring period August 1990–May 2000 (54.9813 kg · y or 723.44 mol · y), published recently, are analyzed using the potential of the Bayesian method for low counting rates. First evidence for neutrinoless double beta decay is observed giving first evidence for lepton number violation and for a Majorana nature of the neutrino on a 97 % confidence level. The half-life of the process, found with the Bayesian method, is $T^{0\nu}_{1/2} = (0.8\text{–}18.3) \cdot 10^{25}$ y (95 % C. L.) with the best value of $1.5 \cdot 10^{25}$ y. The value of the effective neutrino mass, deduced with the nuclear matrix elements from [1,2], is $\langle m \rangle = (0.11\text{–}0.56)$ eV (95 % C. L.), with the best value of 0.39 eV. Uncertainties in the nuclear matrix elements may widen the range given for the effective neutrino mass by at most a factor of 2.

С помощью метода Байеса для случая малых скоростей счета событий проанализированы опубликованные недавно данные эксперимента HEIDELBERG–MOSCOW по поиску двойного бета-распада, полученные за время измерений с августа 1990 г. по май 2000 г. (54,9813 кг · год или 723,44 молей · год). При уровне достоверности 97 % обнаружено первое свидетельство безнейтринной моды двойного бета-распада, что, в свою очередь, является первым свидетельством нарушения закона сохранения лептонного числа и первым указанием на майорановскую природу нейтрино. Полученный методом Байеса полупериод этого процесса равен $T^{0\nu}_{1/2}$ =(0,8–18,3) $\cdot 10^{25}$ лет (95 % C. L.) при среднем значении $1,5 \cdot 10^{25}$ лет. Найденное на этой основе с помощью ядерных матричных элементов из [1, 2] значение эффективной массы нейтрино равно $\langle m \rangle$ =(0,11–0,56) эВ (95 % C. L.) при среднем значении 0,39 эВ. Неопределенности использованных матричных элементов могут привести к уширению приведенной области возможных значений эффективной массы нейтрино не более чем в 2 раза.

INTRODUCTION

The neutrino-oscillation interpretation of the atmospheric and solar neutrino data, delivers a strong indication for a nonvanishing neutrino mass. While such kind of experiments yields information on the difference of squared neutrino mass eigenvalues and on mixing angles, the absolute scale of the neutrino mass is still unknown. Information from double beta decay experiments is indispensable to solve these problems [3,4]. Another important problem is that of the fundamental character of the neutrino, whether it is a Dirac or a Majorana particle [5,6]. Neutrinoless double beta decay could answer also this question. Perhaps the main problem,

[1] Spokesman of the HEIDELBERG–MOSCOW and GENIUS Collaborations, e-mail: klapdor@gustav.mpi-hd.mpg.de, hom page: http://www.mpi-hd.mpg.de/non_acc/

which can be investigated by double beta decay with high sensitivity, is that of lepton number conservation or nonconservation.

Double beta decay, the rarest known nuclear decay process, can occur in different modes:

$$2\nu\beta\beta \text{ decay:} \quad A(Z,N) \rightarrow A(Z+2,N-2) + 2e^- + 2\bar{\nu}_e, \tag{1}$$

$$0\nu\beta\beta \text{ decay:} \quad A(Z,N) \rightarrow A(Z+2,N-2) + 2e^-, \tag{2}$$

$$0\nu(2)\chi\beta\beta \text{ decay:} \quad A(Z,N) \rightarrow A(Z+2,N-2) + 2e^- + (2)\chi. \tag{3}$$

While the two-neutrino mode (1) is allowed by the Standard Model of particle physics, the neutrinoless mode ($0\nu\beta\beta$) (2) requires violation of lepton number ($\Delta L = 2$). This mode is possible only if the neutrino is a Majorana particle, i. e., the neutrino is its own antiparticle (E. Majorana [5], G. Racah [6], for subsequent works we refer to [8–10], for some reviews see [4, 11–15]). First calculations of the $0\nu\beta\beta$ decay based on the Majorana theory have been done by W. H. Furry [7].

Neutrinoless double beta decay cannot only probe a Majorana neutrino mass, but various new physics scenarios beyond the Standard Model, such as R-parity violating supersymmetric models, R-parity conserving SUSY models, leptoquarks, violation of Lorentz invariance, and compositeness (for a review see [4, 16, 17]). Any theory containing lepton number violating interactions can in principle lead to this process allowing one to obtain information on the specific underlying theory. The experimental signature of the neutrinoless mode is a peak at the Q value of the decay.

The unique feature of neutrinoless double beta decay is that a measured half-life allows one to deduce information on the effective Majorana neutrino mass $\langle m \rangle$, which is a superposition of neutrino mass eigenstates [11, 12]:

$$[T^{0\nu}_{1/2}(0^+_i \rightarrow 0^+_f)]^{-1} = C_{mm}\frac{\langle m\rangle^2}{m_e^2} + C_{\eta\eta}\langle\eta\rangle^2 + C_{\lambda\lambda}\langle\lambda\rangle^2 + C_{m\eta}\langle\eta\rangle\frac{\langle m\rangle}{m_e} + \\ + C_{m\lambda}\langle\lambda\rangle\frac{\langle m_\nu\rangle}{m_e} + C_{\eta\lambda}\langle\eta\rangle\langle\lambda\rangle, \tag{4}$$

$$\langle m\rangle = |m^{(1)}_{ee}| + \mathrm{e}^{i\phi_2}|m^{(2)}_{ee}| + \mathrm{e}^{i\phi_3}|m^{(3)}_{ee}|, \tag{5}$$

where $m^{(i)}_{ee} \equiv |m^{(i)}_{ee}|\exp(i\phi_i)$ $(i = 1, 2, 3)$ are the contributions to $\langle m\rangle$ from individual mass eigenstates, with ϕ_i denoting relative Majorana phases connected with CP violation, and C_{mm}, $C_{\eta\eta}, ...$ denote nuclear matrix elements, which can be calculated (see, e. g., [1], for a review see, e. g., [4, 12, 13, 18, 19]). Ignoring contributions from right-handed weak currents on the right-hand side of Eq. (4), only the first term remains.

The effective mass is closely related to the parameters of neutrino oscillation experiments, as can be seen from the following expressions

$$|m^{(1)}_{ee}| = |U_{e1}|^2 m_1, \tag{6}$$

$$|m_{ee}^{(2)}| = |U_{e2}|^2 \sqrt{\Delta m_{21}^2 + m_1^2}, \tag{7}$$

$$|m_{ee}^{(3)}| = |U_{e3}|^2 \sqrt{\Delta m_{32}^2 + \Delta m_{21}^2 + m_1^2}\,. \tag{8}$$

Here, U_{ei} are entries of the neutrino mixing matrix, and $\Delta m_{ij}^2 = |m_i^2 - m_j^2|$, with m_i denoting neutrino mass eigenstates. U_{ei} and Δm^2 can be determined from the neutrino oscillation experiments.

The importance of $\langle m \rangle$ for solving the problem of the neutrino mixing matrix structure and in particular to fix the absolute scale of the neutrino mass spectrum, which cannot be fixed by ν-oscillation experiments alone, has been discussed in detail in, e. g., [3, 20, 21].

Double beta experiments to date gave only *upper limits* for the effective mass. The most sensitive limits [22–24] were *already* of striking importance for neutrino physics, excluding, for example, in hot dark matter models, the small mixing angle (SMA) MSW solution of the solar neutrino problem [3, 4, 25–29] in degenerate neutrino mass scenarios.

The HEIDELBERG–MOSCOW double beta decay experiment in the Gran Sasso Underground Laboratory [4, 16, 30–33] searches for double beta decay of $^{76}\mathrm{Ge} \to {}^{76}\mathrm{Se} + 2e^- + {} + (2\bar{\nu})$ since 1990. It is the most sensitive double beta experiment since almost eight years now. The experiment operates five enriched (to 86 %) high-purity ^{76}Ge detectors, with a total mass of 11.5 kg, the active mass of 10.96 kg, being equivalent to a source strength of 125.5 mol ^{76}Ge nuclei. This is the largest source strength in use.

The high energy resolution of the Ge detectors assures that there is no background for a $0\nu\beta\beta$ line from the two-neutrino double beta decay in this experiment.

In this paper, we present a new, refined analysis of the data obtained in the HEIDELBERG–MOSCOW experiment during the period August 1990–May 2000 which have recently been published [24]. The analysis concentrates on the neutrinoless decay mode which is the one relevant for particle physics (see, e. g., [4]). First evidence for the neutrinoless decay mode will be presented. A short communication has been given already in [34].

1. EXPERIMENTAL SET-UP AND RESULTS

A detailed description of the HEIDELBERG–MOSCOW experiment has been given recently in [24, 35]. Therefore only some important features will be given here.

All detectors, whose technical parameters are given in Table 1 (see [35]), except detector No. 4, are operated in a common Pb shielding of 30 cm, which consists of an inner shielding of 10 cm radiopure LC2-grade Pb followed by 20 cm of Boliden Pb. The whole set-up is placed in an air-tight steel box and flushed with radiopure nitrogen in order to suppress the ^{222}Rn contamination of the air. The steel box is centered inside a 10 cm boron-loaded polyethylene shielding to decrease the neutron flux from outside. An active anticoincidence shielding is placed on the top of the set-up to reduce the effect of muons. Detector No. 4 is installed in a separate set-up, which has an inner shielding of 27.5 cm electrolytical Cu, 20 cm lead, and boron-loaded polyethylene shielding below the steel box, but no muon shielding. To check the stability of the experiment, a calibration with a ^{228}Th and a $^{152}\mathrm{Eu} + {}^{228}\mathrm{Th}$, and a ^{60}Co source is done weekly. High voltage of the detectors, temperature in the detector cave and the computer room, the nitrogen flow in the detector boxes, the muon anticoincidence

Table 1. **Technical parameters of the five enriched detectors**

Detector number	Total mass, kg	Active mass, kg	Enrichment in ^{76}Ge, %	FWHM* 1996 at 1332 keV, keV	FWHM* 2000 at 1332 keV, keV
No. 1	0.980	0.920	85.9 ± 1.3	2.22 ± 0.02	2.42 ± 0.22
No. 2	2.906	2.758	86.6 ± 2.5	2.43 ± 0.03	3.10 ± 0.14
No. 3	2.446	2.324	88.3 ± 2.6	2.71 ± 0.03	2.51 ± 0.16
No. 4	2.400	2.295	86.3 ± 1.3	2.14 ± 0.04	3.49 ± 0.24
No. 5	2.781	2.666	85.6 ± 1.3	2.55 ± 0.05	2.45 ± 0.11

*FWHM — full width at half maximum.

signal, leakage current of the detectors, overall and individual trigger rates are monitored daily. The energy spectrum is taken in 8192 channels in the range from threshold up to about 3 MeV, and in a parallel spectrum up to about 8 MeV.

Because of the big peak-to-Compton ratio of the large detectors, external γ activities are relatively easily identified, since their Compton continuum is to a large extent shifted into the peaks. The background identified by the measured γ lines in the background spectrum consists of: 1) primordial activities of the natural decay chains from ^{238}U, ^{232}Th, and ^{40}K, 2) anthropogenic radio nuclides, like ^{137}Cs, ^{134}Cs, ^{125}Sb, ^{207}Bi, 3) cosmogenic isotopes, produced by activation due to cosmic rays. The activity of these sources in the set-up is measured directly and can be located due to the measured and simulated relative peak intensities of these nuclei. Hidden in the continuous background are the contributions of: 4) the bremsstrahlungs spectrum of ^{210}Bi (daughter of ^{210}Pb), 5) elastic and inelastic neutron scattering, and 6) direct muon-induced events.

External α and β activities are shielded by the 0.7 mm inactive zone of the p-type Ge detectors on the outer layer of the crystal. The enormous radiopurity of HP-germanium is proven by the fact that the detectors No. 1, 2 and 3 show no indication of any α peaks in the measured data. Therefore no contribution of the natural decay chains can be located inside the crystals. Detectors No. 4 and 5 seem to be slightly contaminated with ^{210}Pb on the level of few μBq/kg, most likely surface contaminations at the inner contact. This contamination was identified by a measured α peak in the background spectrum at 5.305 MeV of the daughter ^{210}Po and the constant time development of the peak counting rate. There is no contribution to the background in the interesting evaluation areas of the experiment due to this activity. For further details about the experiment and background we refer to [35, 36] (see also Table 2).

In the vicinity of the Q-value of the double beta decay, which has been recently measured with very high precision [37,38] to be $Q_{\beta\beta}$ = 2039.006(50) keV, very weak lines at 2034.744 and 2042 keV from the cosmogenic nuclide ^{56}Co, and from ^{214}Bi (^{238}U-decay chain) at 2010.7, 2016.7, 2021.8 and 2052.9 keV, may in principle be expected.

On the other hand, there are no background γ lines at the position of an expected $0\nu\beta\beta$ line, according to our Monte Carlo analysis of radioactive impurities in the experimental set-up [36] and according to the compilations in [39].

Table 2. **Development of the experimental set-up and of the background numbers in the different data acquisition periods for the enriched detectors of the HEIDELBERG–MOSCOW experiment**

Detector number	Lifetime, days	Date Start End	Shielding			Background*, counts/keV·y·kg	PSA
			Cu	Pb	boron-poly.	2000–2100, keV	
No. 1	387.6	8/90–8/91	yes			0.56	no
		1/92–8/92					no
No. 2	225.4	9/91–8/92		yes		0.29	no
Common shielding for three detectors							
No. 1	382.8	9/92–1/94		yes		0.22	no
No. 2	383.8	9/92–1/94		yes		0.22	no
No. 3	382.8	9/92–1/94		yes		0.21	no
No. 1	263.0	2/94–11/94		yes	yes	0.20	no
No. 2	257.2	2/94–11/94		yes	yes	0.14	no
No. 3	263.0	2/94–11/94		yes	yes	0.18	no
Full Set-up Four detectors in common shielding, one detector separate							
No. 1	203.6	12/94–8/95		yes	yes	0.14	no
No. 2	203.6	12/94–8/95		yes	yes	0.17	no
No. 3	188.9	12/94–8/95		yes	yes	0.20	no
No. 5	48.0	12/94–8/95		yes	yes	0.23	since 2/95
No. 4	147.6	1/95–8/95	yes			0.43	no
No. 1	203.6	11/95–05/00		yes	yes	0.170	no
No. 2	203.6	11/95–05/00		yes	yes	0.122	yes
No. 3	188.9	11/95–05/00		yes	yes	0.152	yes
No. 5	48.0	11/95–05/00		yes	yes	0.159	yes
No. 4	147.6	11/95–05/00	yes			0.188	yes

*Without PSA method.

Figure 1 shows the combined spectrum of the five enriched detectors obtained over the period August 1990–May 2000, with a statistical significance of 54.981 kg · y (723.44 mol · y). The identified background lines give an indication of the stability of the electronics over a decade of measurements. The average rate (sum of all detectors) observed over the measuring time, has proven to be constant within statistical variations. Figure 2 shows the part of the spectrum shown in Fig. 1 in more detail around the Q value of double beta decay. Figure 3 shows the spectrum obtained with detectors No. $1, 2, 3, 5$ over the period August 1990–May 2000, with a significance of 46.502 kg · y. Figure 4 shows the spectrum of single site

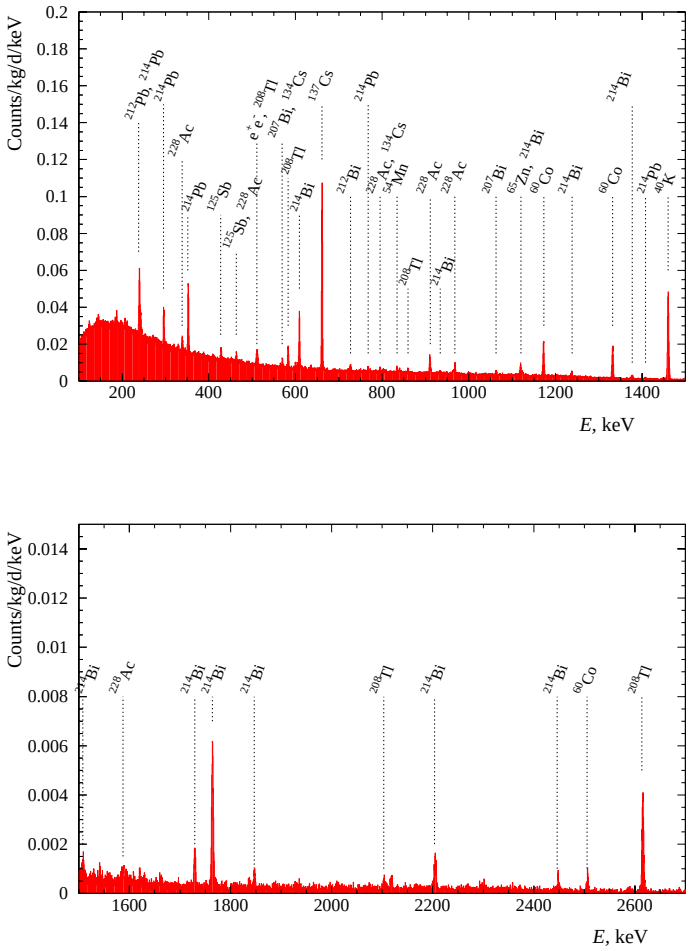

Fig. 1. Sum spectrum of enriched detectors No. 1–5 over the period August 1990–May 2000 (54.9813 kg · y) measured in the HEIDELBERG–MOSCOW experiment. The sources of the main identified background lines are noted

events (SSE) obtained for detectors 2, 3, 5 in the period November 1995–May 2000, under the restriction that the signal simultaneously fulfills the criteria of *all three* methods of pulse-shape analysis we have recently developed [40, 41] and with which we operate all detectors except detector 1 (significance 28.053 kg · y) since 1995.

Double beta events are single site events confined to a few mm region in the detector corresponding to the track length of the emitted electrons. In all three methods, mentioned above, the output of the charge-sensitive preamplifiers was differentiated with 10–20 ns sampled with 250 MHz and analyzed off-line. The methods differ in the analysis of the measured pulse shapes. The first one relies on the broadness of the charge pulse maximum, the second and third one are based on neural networks. All three methods are «calibrated» with known

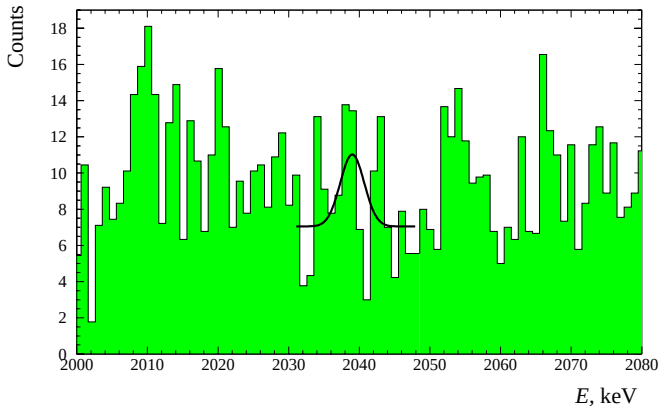

Fig. 2. Sum spectrum of the ^{76}Ge detectors No. 1–5 over the period from August 1990 to May 2000 (54.9813 kg · y) in the energy interval 2000–2080 keV, around the $Q_{\beta\beta}$ value of double beta decay ($Q_{\beta\beta}$ = 2039.006(50) keV) summed to 1 keV bins. The curve results from Bayesian inference in the way explained in Sec. 2. It corresponds to a half-life $T^{0\nu}_{1/2} = (0.80\text{–}35.07) \cdot 10^{25}$ y (95 % C. L.)

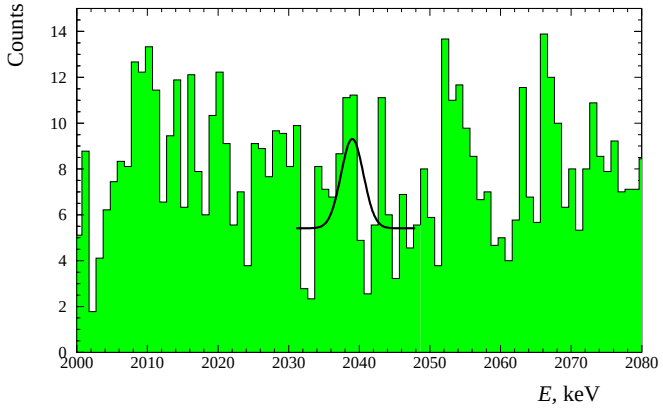

Fig. 3. Sum spectrum of the ^{76}Ge detectors No. 1, 2, 3, 5 over the period from August 1990 to May 2000 (46.502 kg · y), summed to 1 keV bins. The curve results from Bayesian inference in the way explained in Sec. 2. This method leads to the following value for the half-life: $T^{0\nu}_{1/2}$ =(0.75–18.33) · 10^{25} y (95 % C. L.)

double escape (mainly SSE) and total absorption (mainly MSE) γ lines [36, 40–42]. They allow one to achieve about 80 % detection efficiency for both interaction types.

The expectation for a $0\nu\beta\beta$ signal would be a line of single site events on some background of multiple site events but also single site events, the latter coming to a large extent from

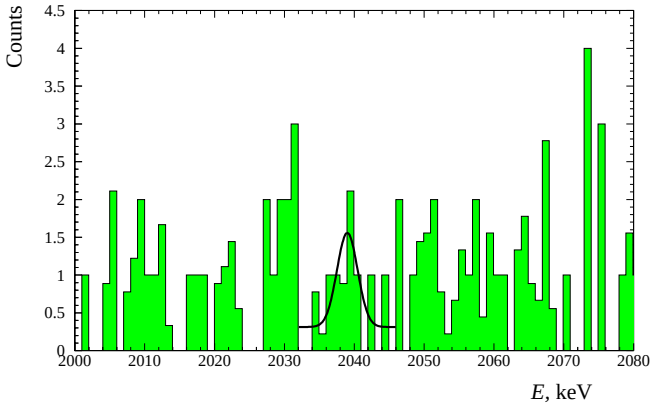

Fig. 4. Sum spectrum of single site events, measured with the detectors No. 2, 3, 5 operated with pulse shape analysis in the period from November 1995 to May 2000 (28.053 kg · y), summed to 1 keV bins. Only events identified as single site events (SSE) by all three pulse shape analysis methods [40–42] have been accepted. The curve results from Bayesian inference in the way explained in Sec. 2. When corrected for the efficiency of SSE identification (see text), this leads to the following value for the half-life: $T^{0\nu}_{1/2} =$ (0.88–22.38) $\cdot 10^{25}$ y (90 % C. L.).

the continuum of the 2614 keV γ line from ^{208}Tl (see, e. g., the simulation in [40]). From simulation we expect that about 5 % of the double beta single site events should be seen also as MSE. This is caused by bremsstrahlung of the emitted electrons [36].

Installation of PSA has been performed in 1995 for the four large detectors. Detector No. 5 runs since February 1995; detectors 2–4, since November 1995 with PSA. The measuring time with PSA from November 1995 until May 2000 is 36.532 kg · y, for detectors 2, 3, 5 it is 28.053 kg · y.

Figure 5 shows typical SSE and MSE events from our spectrum.

All the spectra are obtained after rejecting coincidence events between different Ge detectors and events coincident with activation of the muon shield. The spectra, which are taken in bins of 0.36 keV, are shown in Figs. 2–4 in 1 keV bins, which explains the broken number in the ordinate. We do the analysis of the measured spectra with (Fig. 2) and without the data of detector 4 (Figs. 3, 4) since the latter does not have a muon shield and has the weakest energy resolution. The 0.36 keV bin spectra are used in all analyses described in this work. We ignore for each detector the first 200 days of operation, corresponding to about three half-lives of ^{56}Co ($T_{1/2}$ = 77.27 days), to allow for some decay of short-lived radioactive impurities.

The background rate in the energy range 2000–2080 keV is found to be (0.17 $\pm$ 0.01) events/ kg · y· keV (*without* pulse shape analysis) considering *all* data as background. This is the lowest value obtained in such type of experiments. The energy resolution at the $Q_{\beta\beta}$ value in the sum spectra (Figs. 2–4) is extrapolated from the strong lines in the spectrum to be (4.00 $\pm$ 0.39) keV in the spectra with detector 4, and (3.74 $\pm$ 0.42) keV (FWHM) in the spectra without detector 4. The energy calibration of the experiment has an uncertainty of 0.20 keV.

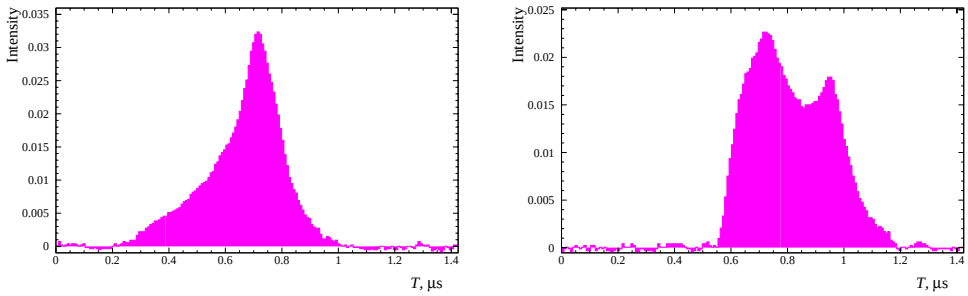

Fig. 5. *a*) Shape of one candidate for $0\nu\beta\beta$ decay (energy 2038.61 keV) classified as SSE by all three methods of pulse shape discrimination. *b*) Shape of one candidate (energy 2038.97 keV) classified as MSE by all three methods

2. DATA ANALYSIS

We analyse the spectra shown in Figs. 2–4 with the following methods:

1. *Bayesian inference*, which is used widely at present in nuclear and astrophysics (see, e. g., [43,44]). This method is particularly suited for low counting rates, where the data follow a Poisson distribution, that cannot be approximated by a Gaussian (see, also [45,46]).

2. *Method recommended by the Particle Data Group* [47]. The χ^2 method is not used since it is expected to have some limitation for application at low counting rates, as also the Maximum Likelihood Method. The limitation is due to the Gaussian approximations inherent in these methods. For the χ^2 method, the Gaussian basis is obvious, for Maximum Likelihood see below.

The Bayesian method is described in the next Subsec. 2.1 (see Appendix). The results from both, Bayesian inference and the recommendation by the Particle Data Group, are given in Sec. 2.2.

2.1. The Bayesian Method. We first describe the procedure summarily and then give some mathematical details.

One knows that the lines in the spectrum are Gaussians with the standard deviation $\sigma = 1.70$ keV in Fig. 2 and $\sigma = 1.59$ keV in Figs. 3, 4. This corresponds to 4.0(3.7) keV FWHM. Given the position of a line, we used Bayes theorem to infer the contents of the line and the level of a constant background.

Bayesian inference yields the joint probability distribution for both parameters. Since we are interested in the contents of the line, the other parameter was integrated out. This yields the distribution of the line contents. If the distribution has its maximum at zero contents, only an upper limit for the contents can be given and the procedure does not suggest the existence of a line. If the distribution has its maximum at nonzero contents, the existence of a line is suggested and one can define the probability K_E that there is a line with nonzero contents.

We define the Bayesian procedure in some more detail. It starts from the distribution $p(x_1 ... x_M|\rho, \eta)$ of the count rates $x_1 ... x_M$ in the bins $1 ... M$ of the spectrum — given two

parameters ρ, η. The distribution p is the product

$$p(x_1 ... x_M|\rho,\eta) = \prod_{k=1}^{M} \frac{{\lambda_k}^{x_k}}{x_k!} \mathrm{e}^{-\lambda_k} \tag{9}$$

of Poissonians for the individual bins. The expectation value λ_k is the superposition

$$\lambda_k = \rho[\eta f_1(k) + (1-\eta) f_2(k)] \tag{10}$$

of the form factors f_1 of the line and f_2 of the background, i. e., f_1(k) is the Gaussian centered at E with the above-mentioned standard deviation value and $f_2(k) \equiv f_2$ is a constant. Note that the model allows for a spectrum of background *only*, i. e., $\eta = 0$.

Since

$$\sum_{k=1}^{M} f_\nu(k) = 1 \text{ for } \nu = 1, 2, \tag{11}$$

one has

$$\sum_{k=1}^{M} \lambda_k = \rho. \tag{12}$$

Hence, ρ parametrizes the total intensity in the spectrum, and η is the relative intensity in the Gaussian line.

The total intensity ρ shall be integrated out. For this purpose, one needs the prior distribution $\mu(\rho|\eta)$ of ρ for fixed η. We obtain it from Jeffreys' rule (§ 5.35 of [44]).

$$\mu(\rho \,|\, \eta) = \left| \overline{\frac{\partial^2}{\partial \rho^2} \ln p} \right|^{1/2}. \tag{13}$$

The overline denotes the expectation value with respect to $x_1 ... x_M$. The integration

$$p_1(x_1 ... x_M|\,\eta) \sim \int d\rho \, p(x_1 ... x_M \,|\, \rho, \eta) \, \mu(\,\rho \,|\, \eta) \tag{14}$$

then yields the model p_1 conditioned by η alone. It is normalized to unity and the prior distribution

$$\mu_1(\eta) = \left| \overline{\frac{\partial^2}{\partial \eta^2} \ln p_1} \right|^{1/2} \tag{15}$$

of η is obtained by application of Jeffrey's rule to p_1. Bayes' theorem yields the posterior distribution

$$P_1(\eta|x_1 ... x_M) = \frac{p_1(x_1 ... x_M|\,\eta)\,\mu_1(\eta)}{\int d\eta \, p_1 \, \mu_1} \tag{16}$$

of η.

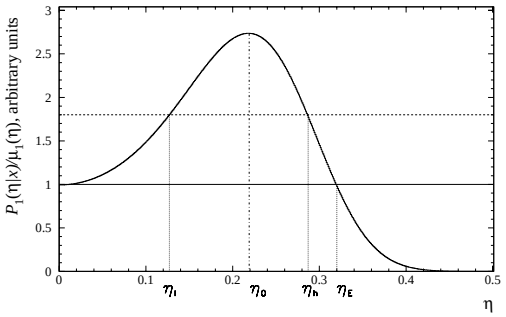

Fig. 6. The figure shows the relation between P_1, K, and K_E. K is the integral over P_1 in the limits $[\eta_l, \eta_h]$. The integral over P_1 in the interval [0, η_E] is K_E

From the posterior the «error interval» for η is obtained. It is the shortest interval in which η lies with probability K. The length of an interval is defined with the help of the measure $\mu_1(\eta)$. We call this the Bayesian interval for the probability K in order to distinguish it from a confidence interval of classical statistics. There is a limit, where Bayesian intervals agree with confidence intervals. See below.

The borders of a Bayesian interval are given by the intersections of the likelihood function $P_1(\eta \,|\, x)/\mu_1(\eta) \sim p_1(x|\eta)$ with a horizontal line at η_l, η_h (Fig. 6). The probability K is obtained by integrating P_1 from η_l to η_h.

When the likelihood function has its maximum at $\eta = 0$, then the Bayesian interval will — for every K — include $\eta = 0$. Then this value cannot be excluded and only an upper limit for the contents of the line can be given.

When the maximum of the likelihood function is at a point different from $\eta = 0$ — as it is in Fig. 6 — then there is a range of K values such that the associated interval excludes the point $\eta = 0$. Under this condition let us construct the interval that has its lower border at $\eta = 0$. It extends up to η_E. The associated probability is called K_E. The point $\eta = 0$ now limits the possible η values in a nontrivial way because for every $K < K_E$, the associated error interval *excludes* zero. We call K_E the probability that there exists a line.

The above considerations lead to a peak finding procedure. One can prescribe a line at an arbitrary energy E of the spectrum — say of Fig. 2 — and determine the probability K_E that there is one. Such searches lead to the results given in the next section.

Let us note that classical and Bayesian statistics become equal to each other when the likelihood function is well approximated by a Gaussian. In this case, the probability K is the same as classical confidence.

Note that the method of minimum χ^2 is based on an even more stringent limit. It requires Gaussian distributions of the *data*. Since the Gaussian is defined everywhere on the real axis, the method can yield negative values of the parameters, especially negative η in the present case. The Bayesian method respects the natural limitations of the parameters because it accepts non-Gaussian distributions.

The so-called method of maximum likelihood is the Bayesian method with the prior distributions set constant. This is a useful approximation when the posterior is sufficiently

narrow. Then the posterior becomes approximately Gaussian. In this sense, the method of maximum likelihood is based on a hidden Gaussian approximation.

2.2. Results of the Analysis. *2.2.1. The Full Data.* We first concentrate on the full spectra (see Figs. 2, 3) without *any* data manipulation (no background subtraction, no pulse shape analysis). For the evaluation, we consider the *raw data* of the detectors.

The Bayesian peak finding procedure described in the last section has been applied to the spectra of Figs. 2, 3. The result is shown on the left-hand sides of Figs. 7, 8. For every energy E of the spectral range 2000–2080 keV, we have determined the probability K_E that there is a line at E. All the remainder of the spectrum was considered to be background in this search.

The peak detection procedure yields lines at the positions of known weak γ lines from the decay of ^{214}Bi at 2010.7, 2016.7, 2021.8 and 2052.9 keV [39]. In addition, a line centered at 2039 keV shows up. This is compatible with the Q value [37, 38] of the double beta decay process. We emphasize, that at this energy no γ line is expected according to the compilations in [39]. We do not find indications for the lines from ^{56}Co at 2034.7 and 2042 keV discussed earlier [36] (Figs. 7, 8). We have at present no convincing identification of the lines around 2070 keV indicated by the peak identification procedure.

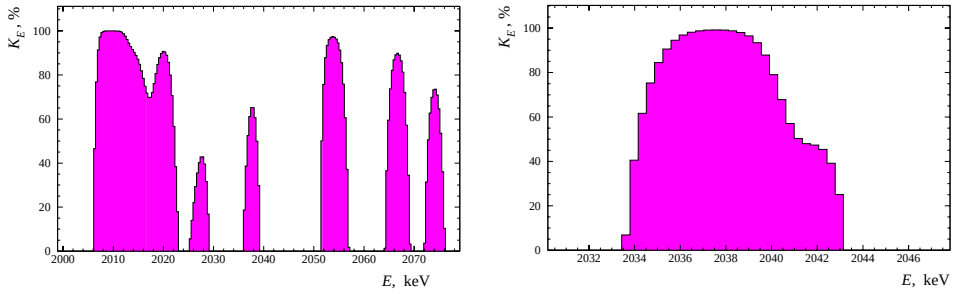

Fig. 7. Scan for lines in the full spectrum taken from 1990–2000 with detectors No. 1–5 (Fig. 2), with the Bayesian method of Sec. 2.1. The ordinate is the probability K_E that a line exists as defined in the text. *a*) Energy range 2000–2080 keV; *b*) energy range of interest for double beta decay

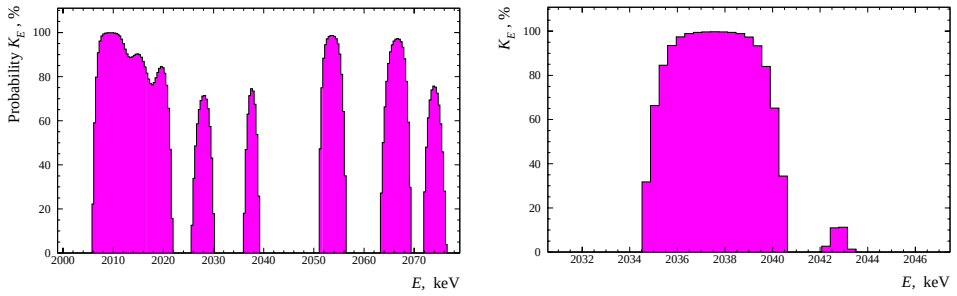

Fig. 8. *a*) Probability K_E that a line exists at a given energy in the range of 2000–2080 keV derived via Bayesian inference from the spectrum shown in Fig. 3. *b*) Result of a Bayesian scan for lines as in (*a*) but in the energy range of interest for double beta decay

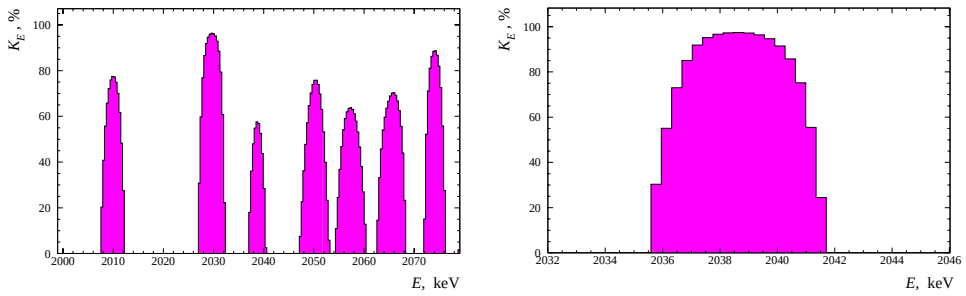

Fig. 9. Scan for lines in the single site event spectrum taken from 1995–2000 with detectors No. 2, 3, 5, (Fig. 4), with the Bayesian method (as in Figs. 7, 8). *a*) Energy range 2000–2080 keV; *b*) energy range of interest around $Q_{\beta\beta}$

Bayesian peak detection suggests a line at $Q_{\beta\beta}$ whether or not one includes detector No. 4 without muon shield (Figs. 7, 8). The line is also suggested in Fig. 9 after removal of multiple site events (MSE), see below.

In Figs. 7, *a*, 8, *a*, 9, *a* the background intensity $(1-\eta)$ identified by the Bayesian procedure is too high because the procedure averages the background over all the spectrum (including lines) except for the line it is trying to single out. Therefore on (*b*) of Figs. 7, 8 (and also Fig. 9) the peak detection procedure is carried out within a smaller energy interval that seems not to contain (according to the left-hand side) lines other than the one at $Q_{\beta\beta}$. Independently of this argument the interval is broad enough (about $\pm$ 5 standard deviations of the Gaussian line) for a meaningful analysis. We find the probability $K_E = 96.5\,\%$ that there is a line at 2039.0 keV in the spectrum shown in Fig. 2. This is a confidence level of 2.1 σ in the usual language. For the spectrum shown in Fig. 3, we find a probability for a line at 2039.0 keV of 97.4 % (2.2 σ). In this case the number of events is found to be 1.2 to 29.4 with 95 % C. L. It is 7.3 to 22.6 events with 68.3 % C. L. The most probable number of events (best value) is 14.8 events. These values are stable against small variations of the interval of analysis. For example, changing the lower and upper limits of the interval of analysis between 2030 and 2032 and 2046 and 2050 yields consistently values of K_E between 95.3 and 98.5 % (average 97.2 %) for the spectrum of Fig. 3.

We also applied the method recommended by the Particle Data Group [47]. This method (which does not use the information that the line is Gaussian) finds a line at 2039 keV on a confidence level of 3.1 σ (99.8 % C. L.).

2.2.2. Single Site Events Data. From the analysis of the single site events (Fig. 4), we find after 28.053 kg · y of measurement 9 SSE events in the region 2034.1–2044.9 keV ($\pm 3\sigma$ around $Q_{\beta\beta}$) (Table 3). Analysis with the Bayesian method of the single site event spectrum (Fig. 4), as described in Sec. 2.1, shows again evidence for a line at the energy of $Q_{\beta\beta}$ (Fig. 9). Analyzing the range of 2032–2046 keV, we find the probability of 96.8 % that there is a line at 2039.0 keV. We thus see a signal of single site events, as expected for neutrinoless double beta decay, precisely at the $Q_{\beta\beta}$ value obtained in the precision experiment of [37]. The analysis of the line at 2039.0 keV before correction for the efficiency yields 4.6 events (best value) or (0.3–8.0) events within 95 % C. L. ((2.1–6.8) events within 68.3 % C. L.). Corrected

Table 3. **Events classified to be single site events (SSE) by all three methods of PSA, in the range 2034.1–2044.9 keV ($\pm 3\sigma$ range around $Q_{\beta\beta}$) of the spectrum taken with enriched detectors No. 2, 3, 5 in the period November 1995–May 2000 (28.053 kg · y)**

No.	N, bin	E, keV	No.	N, Bin	E, keV
1.	5653	2034.66	6.	5666	2039.33
2.	5658	2036.46	7.	5669	2040.41
3.	5660	2037.18	8.	5674	2042.21
4.	5664	2038.61	9.	5680	2044.37
5.	5665	2038.97			

for the efficiency to identify an SSE signal by successive application of all three PSA methods, which is 0.55 ± 0.10, we obtain a $0\nu\beta\beta$ signal with 92.4 % C. L. The signal is (3.6–12.5) events with 68.3 % C. L. (best value 8.3 events).

The PDG method gives a signal at 2039.0 keV of 2.8 σ (99.4 %). The analysis given in Fig. 9, shows partly differences in the relative intensities of other identified lines compared to the full spectra, which should reflect their different composition of single site and multiple site events. This is the subject of further investigation. The possibility that the single site signal is a double escape peak of a γ line at 3021 keV is excluded from the high-energy part of our spectrum.

2.3. Some Comments on the Bayesian, χ^2 and Maximum Likelihood Methods. We probed the sensitivity of peak identification for the three methods: Bayesian, χ^2, Maximum–Likelihood, for the latter two using codes from [48].

The mentioned disadvantage of the latter two methods is that, at low counting rates, observation of lines with negative counting rate is possible. This is *excluded* in the Bayesian method. We find that the Bayesian method yields the most reliable analysis, and also that the Bayesian method tends to systematically give too conservative confidence limits. We shall discuss technical details of the three methods in a separate paper.

3. HALF-LIFE OF THE NEUTRINOLESS MODE AND EFFECTIVE NEUTRINO MASS

We emphasize that we find in all analyses of our spectra a line at the value of $Q_{\beta\beta}$. Under the assumption that the signal at $Q_{\beta\beta}$ is not produced by a presently unknown γ line, we can translate the observed number of events into half-lives. In Table 4 we give conservatively the values obtained with the Bayesian method and not those obtained with the PDG method. Also given in Table 4 are the effective neutrino masses $\langle m \rangle$ deduced using the matrix elements of [1, 2].

We derive from the data taken with 46.502 kg · y the half-life $T^{0\nu}_{1/2} = (0.8\text{–}18.3) \cdot 10^{25}$ y (95 % C. L.). The analysis of the other data sets, shown in Table 4, confirms this result. Of particular importance is that we see the $0\nu\beta\beta$ signal in the single site spectrum.

The result obtained is consistent with the limits given earlier by the HEIDELBERG–MOSCOW experiment [24]. It is also consistent with all other double beta experiments —

Table 4. **Half-life for the neutrinoless decay mode and deduced effective neutrino mass from the HEIDELBERG–MOSCOW experiment**

Significance, kg · y	Detector	$T^{0\nu}_{1/2}$, y	$\langle m \rangle$, eV	Conf. level
54.9813	1, 2, 3, 4, 5	$(0.80–35.07)\cdot 10^{25}$	(0.08–0.54)	95 % C. L.
54.9813	1, 2, 3, 4, 5	$(1.04–3.46)\cdot 10^{25}$	(0.26–0.47)	68 % C. L.
54.9813	1, 2, 3, 4, 5	$1.61\cdot 10^{25}$	0.38	Best Value
46.502	1, 2, 3, 5	$(0.75–18.33)\cdot 10^{25}$	(0.11–0.56)	95 % C. L.
46.502	1, 2, 3, 5	$(0.98–3.05)\cdot 10^{25}$	(0.28–0.49)	68 % C. L.
46.502	1, 2, 3, 5	$1.50\cdot 10^{25}$	0.39	Best Value
28.053	2, 3, 5 SSE	$(0.88–22.38)\cdot 10^{25}$	(0.10–0.51)	90 % C. L.
28.053	2, 3, 5 SSE	$(1.07–3.69)\cdot 10^{25}$	(0.25–0.47)	68 % C. L.
28.053	2, 3, 5 SSE	$1.61\cdot 10^{25}$	0.38	Best Value

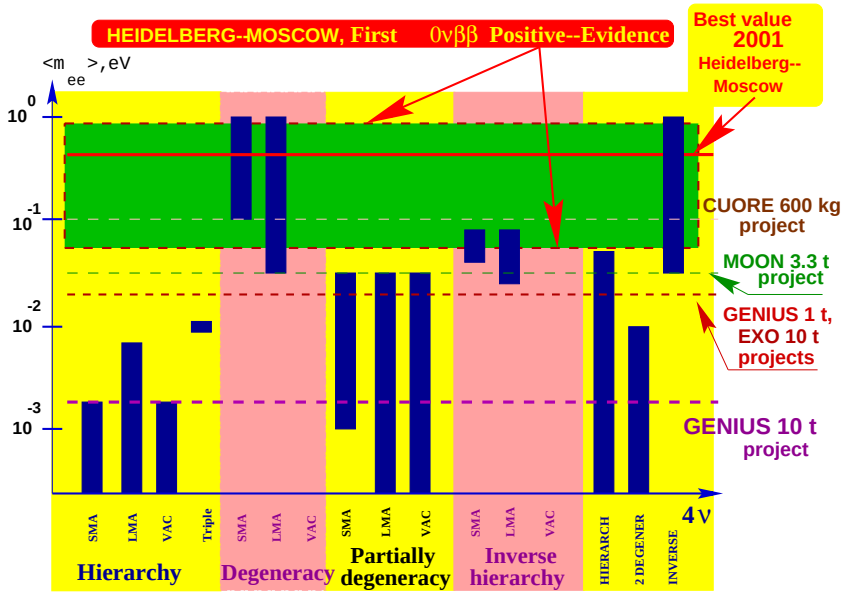

Fig. 10. The impact of the evidence obtained for neutrinoless double beta decay in this paper (best value of the effective neutrino mass $\langle m \rangle$ = 0.39 eV, 95 % confidence range (0.05–0.84) eV — allowing already for an uncertainty of the nuclear matrix element of a factor of ± 50 % on possible neutrino mass schemes. The bars denote allowed ranges of $\langle m \rangle$ in different neutrino mass scenarios, still allowed by neutrino oscillation experiments. Hierarchical models are excluded by the new $0\nu\beta\beta$ decay result. Also shown are the expected sensitivities for the future potential double beta experiments CUORE, MOON, EXO and the 1 ton and 10 ton project of GENIUS [53] from [20]

which still reach less sensitivity. The second Ge experiment [49], which has stopped operation in 1999 after reaching a significance of 9 kg · y, yields (if one believes their method of «visual

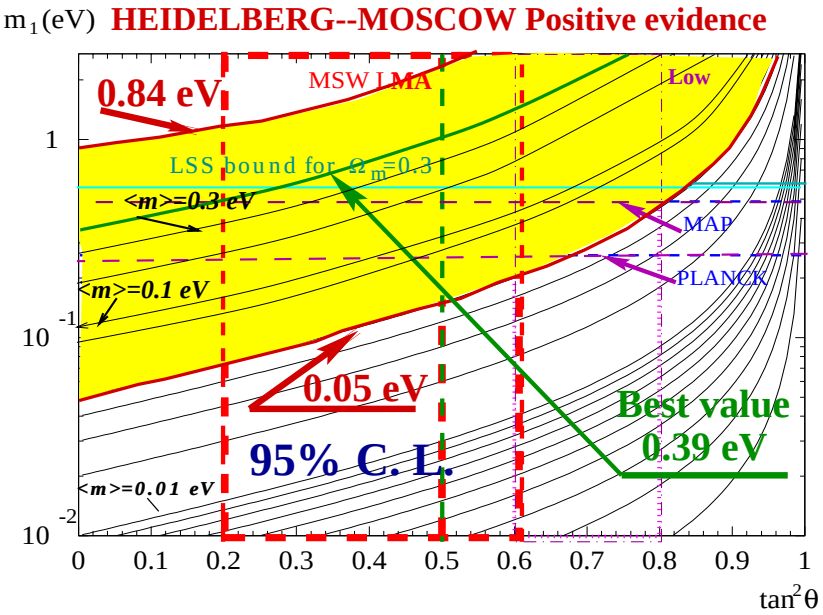

Fig. 11. Double beta decay observable $\langle m \rangle$ and oscillation parameters: the case for degenerate neutrinos. Plotted on the axes are the overall scale of neutrino masses m_0 and mixing $\tan^2 \theta_{12}$. Also shown is a cosmological bound deduced from a fit of CMB and large scale structure [55] and the expected sensitivity of the satellite experiments MAP and PLANCK. The present limit from tritium β decay of 2.2 eV [56] would lie near the top of the figure. The range of $\langle m \rangle$ fixed by the HEIDELBERG–MOSCOW experiment is, in the case of small solar neutrino mixing, already in the range to be explored by MAP and PLANCK

inspection» in their data analysis) in a conservative analysis a limit of $T^{0\nu}_{1/2} > 0.55 \cdot 10^{25}$ y (90 % C. L.). The ^{128}Te geochemical experiment [50] yields $\langle m_\nu \rangle < 1.1$ eV (68 % C. L.), the ^{130}Te cryogenic experiment yields [51] $\langle m_\nu \rangle < 1.8$ eV; and the $CdWO_4$ experiment [52], $\langle m_\nu \rangle < 2.6$ eV, all derived with the matrix elements of [1,19] to make the results comparable to the present value.

Concluding we obtain, with more than 95 % probability, first evidence for the neutrinoless double beta decay mode.

As a consequence, on this confidence level, lepton number is not conserved. Further the neutrino is a Majorana particle. We conclude from the various analyses given above the effective mass $\langle m \rangle$ to be $\langle m \rangle = (0.11\text{–}0.56)$ eV (95 % C. L.), with the best value of 0.39 eV. Allowing conservatively for an uncertainty of the nuclear matrix elements of ± 50 % (for detailed discussions of the status of nuclear matrix elements we refer to [4, 12, 13, 15, 18, 19]) this range may widen to $\langle m \rangle = (0.05\text{–}0.84)$ eV (95 % C. L.).

In this conclusion, it is assumed that contributions to $0\nu\beta\beta$ decay from processes other than the exchange of a Majorana neutrino (see, e. g., [4, 54]) are negligible.

With the limit deduced for the effective neutrino mass, the HEIDELBERG–MOSCOW experiment excludes several of the neutrino mass scenarios allowed from present neutrino

oscillation experiments (see Fig. 10) — allowing mainly only for degenerate mass scenarios, and an inverse hierarchy 3ν and 4ν scenario (the former of these being, however, strongly disfavored by a recent analysis of SN1987A [27]). For details we refer to [20]. In particular, hierarchical mass schemes are excluded at the present level of accuracy.

Assuming the degenerate scenarios to be realized in nature we fix — according to the formulae derived in [3] — the common mass eigenvalue of the degenerate neutrinos to $m = (0.05\text{–}3.4)$ eV. Part of the upper range is already excluded by tritium experiments, which give a limit of $m < 2.2$ eV (95 % C. L.) [56]. The full range can only partly (down to ~ 0.5 eV) be checked by future tritium decay experiments, but could be checked by some future $\beta\beta$ experiments (see, e. g., [4, 53]). The deduced best value lies in a range of interest for Z-burst models recently discussed as explanation for super-high energy cosmic ray events beyond the GKZ-cutoff [57]. The range of $\langle m \rangle$ fixed in this work is, already now, in the range to be explored by the satellite experiments MAP and PLANCK [55, 58] (see Fig. 11).

The neutrino mass deduced allows neutrinos to still play an important role as hot dark matter in the Universe.

New approaches and considerably enlarged experiments (as discussed, e. g., in [53, 59]) will be required in future to fix the neutrino mass with higher accuracy.

Acknowledgements. One of the authors (H. V. Klapdor-Kleingrothaus) would like to thank all colleagues who have contributed to the experiment over the last decade of operation. We are particularly grateful to Dr A. Müller, and Dr F. Petry, Dr B. Maier, Dr J. Hellmig and Dr B. Majorovits who have developed the pulse shape discrimination methods and set up the VME electronics applied in the experiment since 1995. We thank Dr T. Kihm for his highly efficient permanent support in the field of electronics and Dr G. Heusser for his important contribution in the field of low-level techniques. We thank Mr H. Strecker for his invaluable technical contributions. We thank Prof. D. Schwalm for his scientific interest and his efficient support of this project and would like to thank the director of the Gran Sasso Underground Laboratory, Prof. E. Bettini and also the former directors of Gran Sasso Profs. P. Monacelli and E. Bellotti, for invaluable support. Our thanks extend also to the technical staff of the Max-Planck Institut für Kernphysik and of the Gran Sasso Underground Laboratory. We thank Perkin Elmer (former ORTEC) Company, and in particular Dr M. Martini, and Dr R. Collatz for the fruitful cooperation. We are indebted to Prof. H. L. Harney for his cooperation on the Bayesian method. We are grateful to Dr. G. Sawitzki and Prof. W. Beiglböck from the Institute for Applied Mathematics of the University of Heidelberg for encouraging discussions. We acknowledge the invaluable support from BMBF and DFG of this project. We are grateful to the former State Committee of Atomic Energy of the USSR for providing the enriched material used in this experiment.

APPENDIX

To check the Bayes-method of analysing the measured data, and in particular to check the programs we wrote, we have generated spectra and lines with a random number generator and performed then a Bayes analysis. The length of each generated spectrum is 8200 channels, with a line located at bin 5666, the width of the line (sigma) being 4 channels (These special values have been choosen so that every spectrum is analogue to the measured data). The creation of a simulated spectrum is executed in two steps, first the background and second

Table 5. **Results from the analysis of the simulated spectra using a mean background of 4 and 0.5 counts, and different line intensities***

	4 counts				0.5 counts			
Counts	Bayes		Max. Lik.		Bayes		Max. Lik.	
in line	68 %	95 %	68 %	95 %	68 %	95 %	68 %	95 %
0	81	98	60	85	81	99	62	84
5	88	98	68	80	75	100	82	98
10	74	97	74	90	86	100	84	100
20	73	96	77	94	90	100	92	100
100	90	98	87	99	95	100	99	100
200	83	99	78	99	92	100	100	100

*The number d of cases, where the true number of counts in the line (given in the left column), is found in the calculated confidence area is given in the second or third column for the Bayes method, and in the fourth and fifth column for the maximum likelihood method.

the line was created, using random number generators available at CERN (see [48]). In the first step, a Poisson random number generator was used to calculate a random number of counts for each channel, using a mean value of $\mu = 4$ or $\mu = 0.5$, respectively, in the Poisson distribution

$$P(n) = \frac{\mu^n}{n!}\, \mathrm{e}^{-\mu}. \tag{17}$$

These mean values correspond roughly to our mean background measured in the spectra with or without pulse shape analysis.

In the second step, a Gaussian random number generator was used to calculate a random channel number for a Gaussian distribution with a mean value of 5666 (channel) and with a sigma of 4 (channels). The contents of this channel then is increased by one count. This Gaussian distribution filling procedure was repeated for n times, n being the number of counts in this line.

For each choice of μ and n, 100 different spectra were created, and analysed subsequently with two different methods: the maximum likelihood method (using the program set of [48]) and the newly developed Bayes-method. Each method, when analysing a spectrum gives a lower and an upper limit for the number of counts in the line for a given confidence level c (e. g., $c = 95\,\%$) (let us call it *confidence area A*). A confidence level of 95 % means, that in 95 % of all cases the true value should be included in the calculated confidence area. This should be exactly correct when analysing an infinite number of created spectra. When using 100 spectra, as done here, it should be expected that this number is about the same. Now these 100 spectra with a special n and μ are taken to calculate a number d, which is the number of that cases, where the true value n is included in the resulting confidence area A.

This number d is given in Table 5 for the results of the two different analysis methods and for various values for μ and n. It can be seen, that the Bayes method reproduces even the smallest lines properly, while the Maximum Likehood method has some limitations there.

Table 6. **Number of spectra with a calculated confidence limit above a given value**

C. L.	Expected	Found
90.0 %	100 ± 31	96
95.0 %	50 ± 7	42
99.0 %	10 ± 3	12
99.9 %	1 ± 1	0

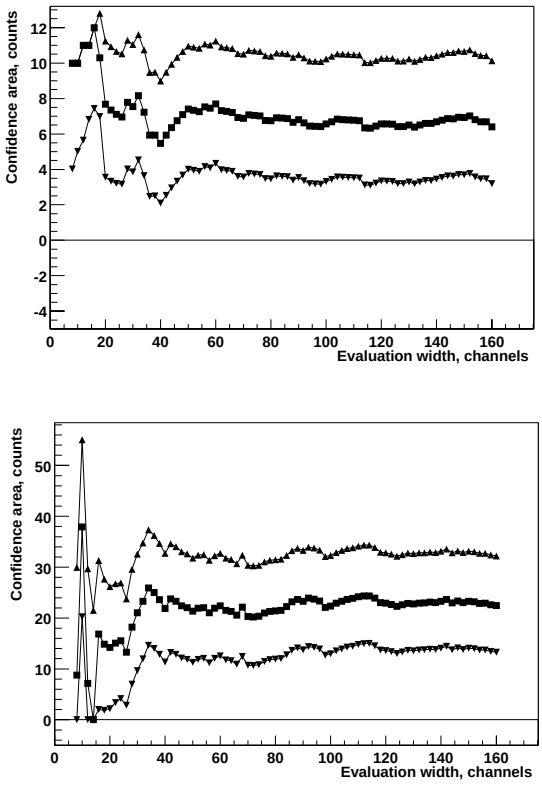

Fig. 12. *a*) Analysis of simulated spectrum with Gaussian peak of 5 events and FWHM of 9.4 channels on a Poisson-distributed background spectrum of 0.5 events/channel, as function of interval of analysis. The middle line is the best value. Upper and lower lines correspond to the 68.3 % confidence limits. *b*) The same as above, but the peak contains 20 events, the background is 4 events/channel. One channel corresponds to 0.36 keV in our measured spectra

Another test has been performed. We generated 1000 simulated spectra containing *no* line. Then the probability has been calculated with the Bayesian method that the spectrum *does* contain a line at a given energy. Table 6 presents the results: the first column contains the corresponding confidence limit c (precisely the parameter K_E defined earlier), the second

column contains the *expected* number of spectra indicating existence of a line with a confidence limit above the value c and the third column contains the number of spectra with a confidence limit above the value c, found in the simulations. The result underlines that K_E here is equivalent to the usual confidence level of classical statistics.

We further investigated with the computer-generated spectra the dependence of the peak analysis on the width of the energy range of evaluation. Two examples are shown in Fig. 12. Here the contents of the simulated peak found with the Bayes method is shown as a function of the analysis interval given in channels (one channel corresponds to 0.36 keV in our measured spectra). The line in the middle is the best-fit value of the method, the upper and lower lines correspond to the upper and lower 68.3 % confidence limits. In the upper figure the true number of counts in the simulated line was 5 events, on a Poisson-distributed background of 0.5 events/channel, in the lower figure it was 20 events on a background of 4 events/channel. It can be seen, that the analysis gives safely the correct number of counts, when choosing an analysis interval of not less than 40 channels.

REFERENCES

1. *Staudt A., Muto K., Klapdor-Kleingrothaus H. V.* // Europh. Lett. 1990. V. 13. P. 31.

2. *Muto K., Bender E., Klapdor-Kleingrothaus H. V.* // Z. Phys. A. 1989. V. 334. P. 187–194.

3. *Klapdor-Kleingrothaus H. V., Päs H., Smirnov A. Yu.* // Phys. Rev. D. 2001. V. 63. P. 073005; hep-ph/0003219. 2000; hep-ph/0103076. 2001; Proc. of the 3rd Intern. Conf. on Dark Matter in Astro- and Particle Physics (DARK2000), Heidelberg, Germany, July 10–16, 2000 / Ed. H. V. Klapdor-Kleingrothaus. Heidelberg, 2001. P. 420–434.

4. *Klapdor-Kleingrothaus H. V.* 60 Years of Double Beta Decay — From Nuclear Physics to Beyond the Standard Model. Singapore, 2001. P. 1281.

5. *Majorana E.* // Nuovo Cim. 1937. V. 14. P. 171–184.

6. *Racah G.* // Nuovo Cim. 1937. V. 14. P. 322–328.

7. *Furry W. H.* // Phys. Rev. 1939. V. 56. P. 1184–1193.

8. *Mclennan J. A.* // Jr. Phys. Rev. 1957. V. 106. P. 821.

9. *Case K. M.* // Phys. Rev. 1957. V. 107. P. 307.

10. *Ahluwalia D. V.* // Int. J. Mod. Phys. A. 1996. V. 11. P. 1855.

11. *Doi M., Kotani T., Takasugi E.* // Prog. of Theor. Phys. Suppl. 1985. V. 83. P. 1–175.

12. *Muto K., Klapdor-Kleingrothaus H. V.* Neutrinos, Graduate Texts in Contemporary Physics / Ed. H. V. Klapdor-Kleingrothaus. Berlin, 1988. P. 183–238.

13. *Grotz K., Klapdor-Kleingrothaus H. V.* Die Schwache Wechselwirkung in Kern-, Teilchen- und Astrophysik. Stuttgart, 1989; The Weak Interaction in Nuclear, Particle and Astrophysics. Bristol, 1990; Moscow, 1992; China, 1998.

14. *Klapdor-Kleingrothaus H. V., Staudt A.* Teilchenphysik ohne Beschleuniger. Stuttgart, 1995; Non-Accelerator Particle Physics. Bristol; Philadelphia, 1995; Translated by V. A. Bednyakov. 2nd edition. M.: Nauka; Fizmalit, 1998.

15. *Vogel P.* Current Aspects of Neutrino Physics / Ed. D. O. Caldwell. Berlin; Heidelberg, 2001. P. 177–198.

16. *Klapdor-Kleingrothaus H. V.* // Int. J. Mod. Phys. A. 1998. V. 13. P. 3953; Proc. of Symp. on Lepton and Baryon Number Violation, Trento, Italy, April 20–25, 1998 / Ed. H. V. Klapdor-Kleingrothaus, I. V. Krivosheina. Bristol, 1999. P. 251–301; hep-ex/9901021.

17. *Klapdor-Kleingrothaus H. V.* // Springer Tracts in Modern Physics. Heidelberg, 2000. V. 163. P. 69–104.

18. *Faessler A., Simkovic F.* // J. Phys. G. 1998. V. 24. P. 2139–2178; hep-ph/9901215; 1999. P. 1–32.

19. *Tomoda T.* // Rept. Prog. Phys. 1991. V. 54. P. 53–126.

20. *Klapdor-Kleingrothaus H. V., Sarkar U.* // Mod. Phys. Lett. A. 2001. V. 17, No. 37. P. 2469–2482.

21. *Vissani F.* // Proc. of the 3rd Intern. Conf. on Dark Matter in Astro- and Particle Physics (DARK2000), Heidelberg, July 10–16, 2000 / Ed. H. V. Klapdor-Kleingrothaus. Heidelberg, 2001. P. 435–447.

22. *HEIDELBERG–MOSCOW Collaboration* // Phys. Lett. B. 1997. V. 407. P. 219–224.

23. *HEIDELBERG–MOSCOW Collaboration* // Phys. Rev. Lett. 1999. V. 83. P. 41–44.

24. *Klapdor-Kleingrothaus H. V. et al. (HEIDELBERG–MOSCOW Collaboration)* // Eur. Phys. J. A. 2001. V. 12. P. 147; hep-ph/0103062; Proc. of Intern. Conf. on Dark Matter in Astro- and Particle Physics (DARK2000). Heidelberg, 2001. P. 520–533.

25. *Georgi H., Glashow S. L.* // Phys. Rev. D. 2000. V. 61. P. 097301; hep-ph/9808293.

26. *Ellis J., Lola S.* // Phys. Lett. B. 1999. V. 458. P. 310; hep-ph/9904279.

27. *Minakata H., Nunokawa H.* // Phys. Lett. B. 2001. V. 504. P. 301–308; hep-ph/0010240.

28. *Minakata H.* hep-ph/0101148.

29. *Minakata H., Yasuda O.* // Phys. Rev. D. 1997. V. 56. P. 1692; hep-ph/9609276.

30. *Klapdor-Kleingrothaus H. V.* Vorschlag eines Experiments. Internal Report. MPI H. 1987. V. 17. 18 p.

31. *Klapdor-Kleingrothaus H. V.* // Proc. of the 18th Conf. on NEUTRINO'98, Takayama, Japan, June 4–9, 1998 / Eds.: Y. Suzuki et al.; Nucl. Phys. (Proc. Suppl.). 1999. V. 77. P. 357–368.

32. *Klapdor-Kleingrothaus H. V.* // Proc. of the Intern. Symp. on Advances in Nuclear Physics / Eds.: D. Poenaru, S. Stoica. Singapore, 2000. P. 123–129.

33. *Klapdor-Kleingrothaus H. V.* // Proc. of the 17th Intern. Conf. «Neutrino Physics and Astrophysics» (NEUTRINO'96), Helsinki, Finland, June 13–19, 1996 / Eds.: K. Enqvist, K. Huitu, J. Maalampi. Singapore, 1997. P. 317–341.

34. *Klapdor-Kleingrothaus H. V. et al.* // Mod. Phys. Lett. A. 2001. V. 16, No. 37. P. 2409–2420; http://www.mpi-hd.mpg.de/non_acc/

35. *Günther M. et al. (HEIDELBERG–MOSCOW Collaboration)* // Phys. Rev. D. 1997. V. 55. P. 54.

36. *Maier B.* Dissertation. Nov. 1995. MPI-Heidelberg;

Petry F. Dissertation. Nov. 1995. MPI-Heidelberg;

Hellmig J. Dissertation. Nov. 1996. MPI-Heidelberg;

Majorovits B. Dissertation. Dec. 2000. MPI-Heidelberg;

Dietz A. Dipl. Thesis. Univ. Heidelberg, 2000 (unpublished); Dissertation (in preparation).

37. *Douysset G. et al.* // Phys. Rev. Lett. 2001. V. 86. P. 4259–4262.

38. *Hykawy J. G. et al.* // Phys. Rev. Lett. 1991. V. 67. P. 1708.

39. *Firestone R. B., Shirley V. S.* Table of Isotopes. 8th edition. N.Y., 1998;

Chu S. Y. F., Ekström L. P., Firestone R. B. The Lund/LBNL Nuclear Data Search. Vers. 2.0. Feb. 1999.

40. *Hellmig J., Klapdor-Kleingrothaus H. V.* // Nucl. Instr. Meth. A. 2000. V. 455. P. 638–644.

41. *Majorovits B., Klapdor-Kleingrothaus H. V.* // Eur. Phys. J. A. 1999. V. 6. P. 463.

42. *Hellmig J., Petry F., Klapdor-Kleingrothaus H. V.* Patent DE19721323A.

43. *D'Agostini G.* hep-ex/0002055;

von der Linden W., Dose V. // Phys. Rev. E. 1999. V. 59. P. 6527;

Fröhner F. H. // JEFF Report. 2000. V. 18; NEA OECD. Nucl. Sci. a. Engineering. 1997. V. 126. P. 1.

44. *O'Hagan A.* Bayesian Inference. V. 2B: Kendall's Advanced Theory of Statistics. London: Arnold, 1994.

45. *Harney H. L.* physics/0103030.

46. *Harney H. L.* Bayesian Inference. Data Evaluation and Decisions. Heidelberg: Springer Verlag, 2002.

47. *Groom D. E. et al. (Particle Data Group)* // Eur. Phys. J. C. 2000. V. 15. P. 1.

48. http://root.cern.ch and http://wwwinfo.cern.ch/asd/lhc++/indexold.html

49. *Aalseth C. E. et al.* (*IGEX Collaboration*) // Yad. Fiz. 2000. V. 63, No. 7. P. 1299–1302.

50. *Bernatowicz T. et al.* // Phys. Rev. Lett. 1992. V. 69. P. 2341–2344; Phys. Rev. C. 1993. V. 47. P. 806–825.

51. *Alessandrello A. et al.* // Phys. Lett. B. 2000. V. 486. P. 13–21.

52. *Danevich F. A. et al.* // Phys. Rev. C. 2000. V. 62. P. 045501.

53. *Klapdor-Kleingrothaus H. V.* hep-ph/0103074; Proc. of the 2nd Workshop on Neutrino Oscillations and Their Origin (NOON2000), Tokyo, Japan, Dec. 6–18, 2000 / Eds. Y. Suzuki et al. 2001;

Klapdor-Kleingrothaus H. V. // Nucl. Phys. (Proc. Suppl.). 2001. V. 100. P. 309–313; hep-ph/0102276;

Klapdor-Kleingrothaus H. V. // Part. Nucl. Lett. 2001. V. 104. P. 20–39; hep-ph/0102319;

Klapdor-Kleingrothaus H. V. // Proc. of the 1st Intern. Conf. on Particle Physics Beyond the Standard Model (BEYOND'97), Ringberg Castle, Germany, June 8–14, 1997 / Ed. by H. V. Klapdor-Kleingrothaus, H. Päs. IOP Bristol, 1998. P. 485–531;

Klapdor-Kleingrothaus H. V. et al. MPI-Report MPI-H-V26-1999; hep-ph/9910205; Proc. of the 2nd Intern. Conf. on Particle Physics Beyond the Standard Model (BEYOND'99), Ringberg Castle, Germany, June 6–12, 1999 / Ed. by H. V. Klapdor-Kleingrothaus, I. V. Krivosheina. IOP Bristol, 2000. P. 915–1014.

54. *Mohapatra R. N., Pal P. B.* Massive Neutrinos in Physics and Astrophysics // World Scientific Lecture Notes in Physics. Singapore, 1991. V. 41. P. 318.

55. *Lopez R. E.* astro-ph/9909414;

Primack J. R., Gross M. A. K. astro-ph/0007165;

Primack J. R. astro-ph/0007187;

Einasto J. // Proc. of DARK2000, Heidelberg, Germany, July 10–15, 2000 / Ed. H. V. Klapdor-Kleingrothaus. Heidelberg, 2001.

56. *Weinheimer C.* // Proc. of 3rd Intern. Conf. on Dark Matter in Astro- and Particle Physics (DARK 2000), Heidelberg, Germany, July 10–16, 2000 / Ed. H. V. Klapdor-Kleingrothaus. Heidelberg, 2001. P. 513–519.

57. *Weiler T. J.* // Proc. of the 2nd Intern. Conf. on Particle Physics Beyond the Standard Model (BEYOND'99), Ringberg Castle, Germany, June 6–12, 1999 / Ed. by H. V. Klapdor-Kleingrothaus, I. V. Krivosheina. IOP Bristol, 2000. P. 1085–1106;

Päs H., Weiler T. J. // Phys. Rev. D. 2001. V. 63. P. 113015; hep-ph/0101091.

58. *Klapdor-Kleingrothaus H. V.* // Prog. Part. Nucl. Phys. V. 48, Issue 1.

59. *Klapdor-Kleingrothaus H. V.* // Proc. of NANP'2001. Part. and Nucl., Lett. 2002 (to be published);

Klapdor-Kleingrothaus H. V. // Proc. of TAUP'01, Gran-Sasso, Italy, Sept. 7–13, 2001 / Eds. A. Bettini et al. 2002.

Received on January 30, 2002.